Photosynthesis Research **68:** 181–192, 2001.

Regular paper

Monochromatic ultraviolet light induced damage to Photosystem II efficiency and carbon fixation in the marine diatom *Thalassiosira pseudonana* (3H)

Joe Grzymski*, Cristine Orrico & Oscar M. Schofield
*Institute of Marine and Coastal Sciences, Rutgers, The State University of New Jersey, 71 Dudley Road, New Brunswick, NJ 08901-8521, USA; *Author for corespondence (e-mail: joeg@imcs.rutgers.edu; fax: +1-732-932-4083)*

Received 13 March 2000; accepted in revised form 26 March 2001

Key words: carbon fixation, fluorescence, Photosystem II, phytoplankton, ultra-violet light

Abstract

Low light adapted cultures of the marine diatom *Thalassiosira pseudonana* (3H) were cultured and incubated for 30 min under different ultraviolet (UV) wavelengths of near monochromatic light with and without background photosynthetically active radiation (PAR, 380–700 nm). Maximum damage to the quantum yield for stable charge separations was found in the UVB (280-320 nm) wavelengths without background PAR light while the damage under PAR was 30% less. UV induced damage to carbon fixation in the cells was described by a function similar to non-linear functions of inhibiting irradiance previously published with the exception that damage was slightly higher in the UVA (320–380). Various measurements of fluorescent transients were measured and the results indicate localised damage most likely on the acceptor side of the Photosystem II reaction center. However, dark adapted measurements of fluorescence transients with and without DCMU do not result in similar functions. This is also true for the relationships between fluorescence transients and carbon fixation for this species of marine diatom. The correlation between the weightings ϵ_H from measurements of carbon fixation and the quantum yield for stable charge separation as calculated from induction curves with DCMU and without DCMU is R^2 0.44 and R^2 0.78, respectively. The slopes of the two measurements are 3.8 and 1.4, respectively. The strong correlation between the weightings of the induction curves without DCMU and carbon fixation are due to a loss of electron transport from the reaction center to plastoquinone. Under these experimental conditions of constant photon flux density (PFD) this is manifested as a strong linear relationship between the decrease in the operational quantum yield of Photosystem II and carbon fixation.

Introduction

The discovery of the ozone hole in Antarctica (Farman et al. 1985) has resulted in concerted efforts to determine the potential impact of elevated levels of ultraviolet-B radiation (UVB, 280–320 nm) on photoautotrophic activity (Smith et al. 1992) and marine organisms, in general (Calkins 1980). The enhancement of UVB can significantly depress both higher plant and microalgal photosynthetic rates (Iwanzik et al. 1983; El-Sayed et al. 1990; Teramura et al. 1991; Helbing et al. 1992; Smith et al. 1992). The magnitude of UV inhibition depends on UV dose and UV dose rate (Cullen and Lesser 1991), and on the measurement techniques utilized (Coohill 1994; Prézelin et al. 1994a). There are also important physiological and structural differences between higher plants and single celled algae. Therefore species-specific differences in sensitivity to UV radiation must be considered (Jokiel and York 1984; Karentz et al. 1991; Helbing et al. 1992; Smith et al. 1992; Karentz 1994; Vernet et al. 1994). Inhibition rates are difficult to interpret especially if the specific target sites of damage are not known. Action spectra (or biological weighting

factors) can provide a quantitative means to estimate the impact of elevated ultraviolet light on natural communities (Smith et al. 1980; Cullen et al. 1992; Quaite et al. 1992) if the underlying processes influencing the photoinhibition are characterized (Coohill 1991).

Action spectra describe the wavelength dependent sensitivity of a process to light-induced damage (Smith et al. 1980; Rundel 1983; Caldwell et al. 1986; Coohill 1989; Cullen et al. 1992). They can be used to discriminate between the photoinhibition due to UVB, ultraviolet-A (UVA, 320–400 nm), and photosynthetically available radiation (PAR, 400–700 nm), all of which impact photosynthetic activity in a differential manner (cf. Helbing et al. 1992; Baker and Bowyer 1994; Prezelin et al. 1994b). Defining processes that influence the spectral variability in action spectra would allow for a mechanistic interpretation of the variability in UVB-induced damage (Coohill 1991). Photoinhibition is a function of both damage and repair processes. Therefore, biological responses to UV are sensitive to dose and dosage rate (i.e., reciprocity does not hold, Cullen and Lesser 1991; Lesser et al. 1994; Neale et al. 1994). This, and that UVB impacts numerous targets contribute to the significant variability observed in the polychromatic action spectra for photosynthesis (Neale et al. 1994; Boucher and Prezelin 1996). Our ability to mechanistically describe this variability will require an understanding of: the specific target sites for UV inhibition within the photosynthetic machinery, the UVB-damage repair rates and the action spectra of repair (within and between species of phytoplankton), and the impact of photoacclimation processes.

Laboratory studies on higher plants and green algae suggest that UVB is most damaging to Photosystem II (PS II) within the photosynthetic machinery (Kulandaivelu and Noorudeen 1983; Iwanzik et al. 1983; Greenberg et al. 1989; Renger et al. 1989). The UVB radiation appears to degrade the D1 protein, part of the D1/D2 heterodimer; the major structural complex within PS II (Greenberg et al. 1989; Richter et al. 1990; Melis et al. 1992; Jansen et al. 1993). Damage to PSII reduces the ability of algae to generate stable charge separations, which results in an overall lowering of carbon fixation rates. Ultra-violet light inhibition of PS II quantum yields has been observed in field communities under the ozone hole (Schofield et al. 1995). These results are to be expected if damage occurs at the primary (Q_A) and/or secondary (Q_B) electron acceptor because the quinones absorb UV wavelengths of light (Greenberg et al. 1989; Melis et al. 1992; Jansen et al. 1993). The donor side of PS II is also a possible target as tyrosines absorb at 280 nm in their reduced form and 310 in their oxidized radical form (Diner and deVitry 1985; Vass et al. 1996). Other studies have demonstrated decreases in the pool size of carbon fixation enzymes such as carbonic anhydrase (Dionisio et al. 1989) and ribulose-1,5-bisphosphate carboxylase/oxygenase (Rubisco) (Strid et al. 1990; Neale et al. 1993). However, the primary targets for the UV-suppression of photosynthetic activity are still debated (Baker et al. 1997).

Our goals in characterizing monochromatic action spectra for a low light adapted culture of *Thalassiosira pseudonana* were to better measure wavelengths of sensitivity to ultraviolet light and to compare the measurements of damage to PS II to depressions to carbon fixation. In areas of the ocean characterized by high mixing rates and potentially high ultraviolet fluxes like the Southern Ocean, phytoplankton damage and repair rates are not in steady state (Neale et al. 1998). The ultimate goal of ocean photo-biology is to reconcile depressions in photosystem II activity and depressions in carbon fixation and the subsequent impact on cellular growth rates. As part of that effort this paper will relate the ultraviolet light impact on non-invasive active fluorescence measurements and carbon fixation.

Materials and methods

Culture conditions

Cultures of the marine diatom *Thalassiosira pseudonana* were grown in temperature controlled incubators at 20 °C. Two identical cultures were grown in 2.8 l fernbach flasks at a light intensity of 80 μmol m^{-2} s^{-1} and were maintained in exponential growth phase by serial dilution with fresh f/2 media (Guillard 1975). Light was provided by Phillips 40CW·RS·WM cool white lamps on a 12:12 h light:dark cycle. Cell numbers and growth rates were determined by cell counting with a Bright Line heamocytometer. The growth rates of the two cultures were the same (Table 1).

Ultraviolet light incubation

Measurements of the spectral sensitivity to ultraviolet light were performed using high intensity light provided by 1000 W xenon arc lamp. Light was directed through a quartz condensing lens and a 1/4 meter monochromator (Oriel Systems). A computer using a

stepper interface controlled the monochromator. Light (2.5 nm full width-half maximum) exiting the monochromator was filtered through a short pass filter (Corion UG 11s) to remove any stray visible light. Experiments on the susceptibility of PS II to ultraviolet light only, were conducted in the absence of visible light. For all incubations, a 1 cm^2 beam of light was focused on a 1 cm quartz cuvette containing 1 ml of culture. The flux of light was measured using a high sensitivity UV-visible 1 cm^2 silicon light detector (Oriel Systems). Cumulative exposure was calculated based on the absorbance at each wavelength and varied between 100 and 200 J m^{-2}. Calibrations of the lamp were repeated throughout the experiment. The sample chamber was also temperature controlled by a circulating water bath.

Fluorescence parameters of
Thalassiosira pseudonana

Baseline measurements of the fluorescence parameters of the phytoplankton cultures were performed in triplicate on the cultures throughout the day. The cultures were probed for PS II efficiency using a *P*ulse *A*mplitude *M*odulated (PAM) fluorometer (Heinz Walz, Effeltrich, Germany). This provided a robust baseline and ensured that changes in PS II efficiency of UV-irradiated cells were not a product of growth conditions or changes in light acclimation. Aliquots of the cultures were dark adapted for 5 min, then fluorescence induction curves with and without 3-(3,4-dichlorophenyl)-1,1-dimethyl urea (DCMU, 20 μm final concentration) and fluorescence decay curves were measured. Calculations of the maximum quantum yield of PS II for stable charge separations are made from measurements of Fo (Q_A, completely oxidised) and Fm (Q_A, completely reduced). The quantum yield as calculated from DCMU induction curves is denoted $\phi_{IIe^\circ(DCMU)}$; while the calculation from Kautsky curves without DCMU is denoted $\phi_{IIe^\circ(Kaut)}$ (Appendix).

Measurements of UV-effect without PAR light

One ml samples of the diatom containing approximately 0.4 μg Chl *a*/ml were incubated for 30 min under 9 wavelengths in the UVB (every 5 nm between 280–320 nm) and 4 wavelengths in the UVA (330, 340, 350, 360). After irradiation, each sample was probed for photosynthetic activity using the PAM fluorometer. Kautsky induction curves without DCMU were measured after triggering a light-emitting diode (665 nm, 30 μmol photons m^{-2} s^{-1}) and a 600 ms flash from a flash lamp (Schott KL-1500). The fluorescence rise was sampled every 300 μs for 4.8 s. The fluorescence transients (O,I,D,P) were determined after smoothing all curves with a 23 point least squares convolution integral (Savitsky and Golay 1964). F_o is the minimum fluorescence level when all the reaction centers are open (Q_A oxidised). F_i is the level corresponding to the reaction centers unable to reduce plastoquinone (Cao and Govindjee 1990). F_d is the subsequent dip in fluorescence and F_p is the maximum level of fluorescence level when all of Q_A, the primary electron acceptor has been reduced (Lavorel 1959; Munday and Govindjee 1969; Govindjee 1995). After the measurements without DCMU samples were dark adapted for 2 min and then incubated for 1 min with DCMU. The induction curve was measured after triggering a 600 ms pulse from a red LED at a sampling rate of 100 μs for 1.6 s. These curves were similarly smoothed and then deconvolved using an exciton-radical pair equilibrium model adapted from Trissl and Lavergne (1994). Examples of both induction curves are presented in Figure 2. Changes in σ_{psII} were calculated from the exciton-radical pair equilibrium model. Briefly, the magnitude of fluorescence can be described as a function of open reaction centers (q):

$$\frac{F}{F_o} = \frac{\frac{F_m}{F_o} - \left(\frac{F_m}{F_o} - (1 + J_{con})\right) \cdot q}{1 + J_{con} \cdot q} \quad (1)$$

The change in open reaction centers over time can further be described by:

$$\frac{dq}{dt} = -\sigma_{II} \cdot q \cdot ((1 + J_{con})/1 + J_{con} \cdot q) \quad (2)$$

Fluorescence decay curves were measured at a resolution of 10 μs for 0.16 s after applying a single turnover flash (Walz, Single Turnover Flash Lamp, XST-103). The fluorescence decay curves describe the reoxidation of Q_A^- by either Q_B or Q_B^- and were quantified by an offset double exponential decay equation:

$$F = A \cdot e^{(-k_a \cdot t)} + B \cdot e^{(-k_b \cdot t)} + F_o \quad (3)$$

In this equation, A and B are amplitudes and k_a and k_b are rate constants for the fast and slow phases respectively. The existence of a slower (t1/2 of 1.5 s) component could not be resolved by the short acquisition time of our setup (0.16 s). Five curves taken 20 s apart were averaged for all decay measurements. The fluorescence induction curves without the addition of

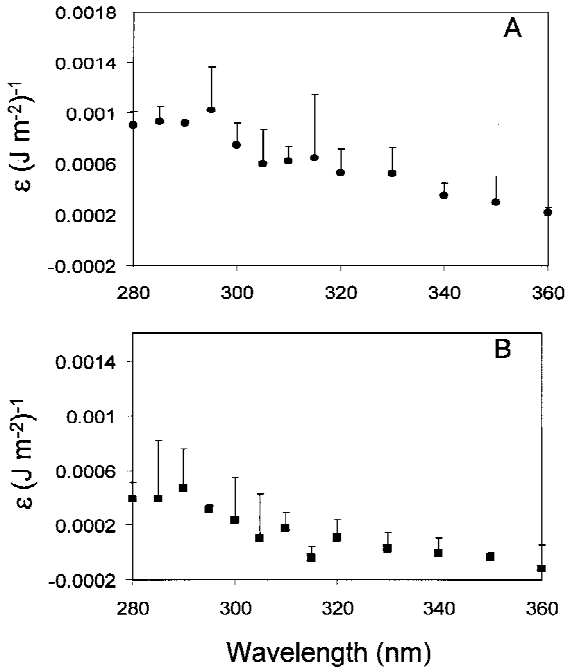

Figure 1. (A) Action spectra of damage to the maximum quantum yield as calculated from induction curves without DCMU $\phi_{\mathrm{IIeo(Kaut)}}$ (circles) after a 30 min incubation under monochromatic UVR only (error bars are the 95% confidence limits, $n > 4$). Calculations of ϵ are explained in the methods. (B) As in A, but as calculated from the maximum quantum yield as calculated from induction curves with DCMU $\phi_{\mathrm{IIeo(DCMU)}}$ (squares).

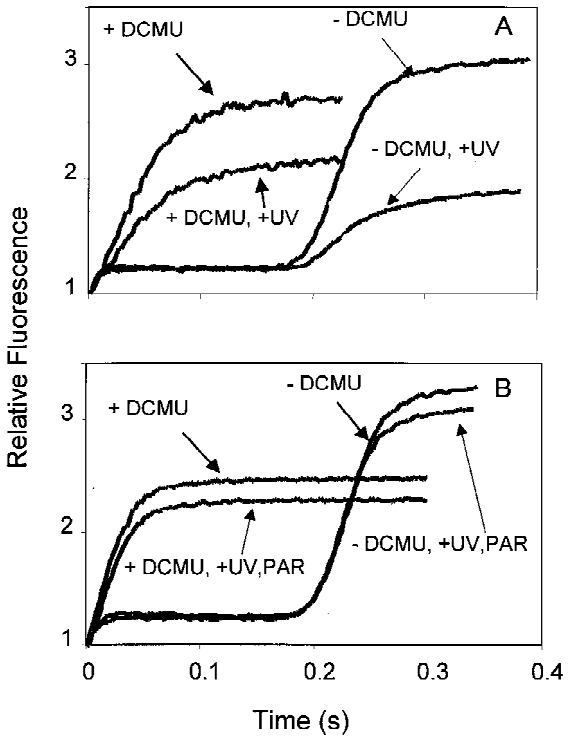

Figure 2. (A) Induction curves with and without DCMU before (grey) and after (black) a 30 min treatment with 300 nm UVR. Curves were normalized to F_o because the majority of the decrease in F_v/F_m was due to changes in F_m. (B) As in A, but after a 30 minute treatment with both 300 nm UVR and 60 μmol photons m^{-2} s^{-1} PAR. The measurements and light intensities of the induction curves are explained in the methods.

DCMU were analyzed for changes in the rise time to the I, D, and P components of the curve as well as the ϕ_I, ϕ_D and ϕ_P. All wavelengths reported were done at least in triplicate.

Analytical measurements in the presence of PAR light

Incubations at 5 wavelengths of UVR (280, 300, 320, 340, 360) and the growth irradiance of the cultures were performed to assess the effect UVR on both PS II efficiency and carbon fixation rates. Aliquots of culture were incubated as described above with one modification: a fiber optic arm providing PAR light (intensity same as growth conditions) was connected to the incubation chamber. At the beginning of each day and periodically throughout the day, controls without UV light were measured in both the incubator and the incubation chamber to assure that deviations were caused by the experimental treatments and not any biological rhythms or changes in the experimental conditions. All fluorescence measurements were also carried out on the controls.

Productivity rates were measured by adding aqueous $NaH^{14}CO_3$ (final concentration of 185 Becquerels l^{-1}) to an aliquot of culture and then irradiating 1 ml samples for the 30 min incubation period. At the end of the incubation period fluorescence measurements in the presence of PAR were made. These included F_o', F_m' and F_t. These values can be used to calculate the efficiency of photon trapping by open PS II centers:

$$\phi_{\mathrm{exc}} = \frac{F_m' - F_o'}{F_m'} \tag{4}$$

The operational quantum yield of PS II can be calculated as:

$$\phi_{\mathrm{PS\ II}} = \frac{F_m' - F_t}{F_m'} \tag{5}$$

After 5 min of dark adaptation the same suite of dark-adapted fluorescence measurements were made as previously described. Samples were then fixed with

10 μl of glacial acetic acid and counted the following day in a scintillation counter (Beckman LS 6000IC). In order to correct for small increases in the chl-*a* content of the sample that occurred during long experiments multiple samples were taken throughout the day. Chlorophyll-*a* content of the cultures was measured in a spectrophotometer (Perkin Elmer, Lambda-12) after an overnight extraction in 100% acetone and dilution with water to a final concentration of 90% acetone. Chlorophyll-*a* content was calculated using the tri-chromatic equation of Jefferies and Humphrey (1975) ($n = 3$).

Calculation of ϵ_H $(J\ m^{-2})^{-1}$

Our short term measurements of the average photosynthetic rate or quantum yield after a specific exposure period of UV with or without PAR light assume no active repair. Therefore the specific weight of inhibition, $\epsilon(\mathrm{J\ m^{-2}})^{-1}$ can be calculated from the cumulative exposure and the average photosynthetic rate (Neale and Kieber 2000):

$$\mathrm{P(t) = P(0)exp - H_{inh}} \tag{6}$$

where:

$$\mathrm{H_{inh} = \epsilon(\lambda)H(\lambda)} \tag{7}$$

and,

$$\epsilon(\lambda) = -\log\left(\frac{\mathrm{P(t)}}{\mathrm{P(0)}}\right)\mathrm{H(\lambda)^{-1}} \tag{8}$$

P(t) is either the measure of Photosystem II activity or carbon fixation initially at the level P(0). H represents the radiant exposure (J m^{-2}) and is calculated based on the measurements of radiant flux in the cuvette filled with water multiplied by the optical density of the sample at the specific wavelength measured.

Results

Acclimation state of T. pseudonana

The cultures of *T. pseudonana* were acclimated to a sub-saturating irradiance (Table 1). Therefore, the maximum rate of light-limited photosynthesis is defined by the ability of the reaction centers and antenna to absorb incoming photons according to a linear function of irradiance with a slope α:

$$\alpha = \sigma_{\mathrm{psu}} \cdot n \cdot \phi_{\mathrm{m}} \tag{9}$$

Table 1. Growth characteristics of *T. pseudonana* (20° C, 12:12 L:D, 80 μmol photons m^{-2} s^{-1}). Production units are μg C μg Chl a^{-1} h^{-1}

Parameter	Value
μ d^{-1}	0.85 ± 0.03
pg chla/ Cell	11.0 ± 1.5
P *versus* I (Chl *a* specific)	
P_{max}	1.83 ± 0.2
α	0.012 ± 0.001
I_k	150 ± 6

where ϕ_{m}:

$$\phi_{\mathrm{m}} = \sigma_{\mathrm{psII}}(\sigma_{\mathrm{psu}})^{-1} \tag{10}$$

Changes therefore, in either σ_{psII} or n, the number of reaction centers, will lead to changes in the maximum rate of light limited photosynthesis at any given light level below I_k (cf. Sakshaug et al. 1997, Appendix). The experimental protocol allowed for close monitoring of changes in σ_{psII} as well as changes in the overall efficiency of generating a stable charge separation, ϕ_{II}. The overall variability in the size of σ_{psII} was 28% and ϕ_{II} varied by less than 10% over the time course of the experiment. Daily variability of σ_{psII} was less than 10%, allowing good resolution in measuring whether or not UVR induced changes in the size of σ_{psII} during experimental treatments.

Signature of Photosystem II damage without PAR

The maximum quantum yield of stable charge separations ($\phi_{\mathrm{IIe}}{}^{\circ}$) declined for both Kautsky and DCMU induction curves after a 30 min treatment with UVR (Figure 1). Both spectra indicate that as wavelength decreases into the UVB damage increases. As well, both spectra also indicate significantly more damage at wavelengths less than 295 nm than in the UVA part of the spectrum ($P < 0.05$); though significant inflections exist in both curves. The decrease in $\phi_{\mathrm{IIe}}{}^{\circ}$ is between 2 and 5 times greater for measurements made without the inhibitor DCMU. These differences are most evident at the lowest wavelengths in the UVB. The differences between the two measurements are obvious when the actual measured curves are overlaid (Figure 2).

Table 2. Calculated fluorescence parameters ± the standard deviation from 30 min treatments with PAR and UVR ($n > 4$). Bold numbers indicate a significant difference from PAR ($P < 0.05$)

Wavelength	ϕ_i	ϕ_d	ϕ_p	a	b	k_a (ms^{-1})	k_b (s^{-1})	$\sigma_{ps\ II}$	J_{con}
PAR	0.159 ± 0.047	0.142 ± 0.049	0.633 ± 0.039	0.422 ± 0.041	0.108 ± 0.059	8.2 ± 1.0	84.8 ± 26.9	52.3 ± 14.4	0.93 ± 0.22
360	0.174 ± 0.045	0.146 ± 0.046	0.637 ± 0.023	0.407 ± 0.039	0.102 ± 0.014	7.3 ± 1.210	7.0 ± 66.2	53.1 ± 7.0	0.97 ± 0.07
340	**0.215 ± 0.034**	**0.184 ± 0.038**	0.619 ± 0.027	0.386 ± 0.053	0.133 ± 0.064	**6.3 ± 1.7**	95.6 ± 45.0	46.6 ± 13.6	**0.83 ± 0.1**
320	**0.202 ± 0.055**	0.173 ± 0.06	**0.610 ± 0.046**	0.410 ± 0.045	0.134 ± 0.058	7.5 ± 1.58	2.1 ± 57.7	40.6 ± 10.2	**0.79 ± 0.12**
300	0.141 ± 0.022	**0.113 ± 0.026**	**0.534 ± 0.051**	0.389 ± 0.046	0.128 ± 0.028	7.9 ± 1.810	8.0 ± 144.7	49.7 ± 17.9	**0.44 ± 0.11**
280	0.141 ± 0.022	**0.113 ± 0.031**	**0.548 ± 0.042**	0.387 ± 0.021	0.116 ± 0.031	7.1 ± 1.2	88.5 ± 52.5	49.9 ± 2.8	**0.54 ± 0.12**

Signature of Photosystem II damage with PAR

Although there is less spectral resolution in the PSII damage curves generated under both UVR and PAR the results were highly repeatable (Table 2). Damage as measured by induction curves with and without DCMU was less in the presence of PAR than under UVR alone. Maximum values of damage under PAR and UVR were 0.0007 and 0.00014 $(J\ m^{-2})^{-1}$ for Kautsky curves and DCMU induction curves respectively (Figure 3). Whereas values were 0.0009 and 0.0004 $(J\ m^{-2})^{-1}$ for the same measurements under UVR alone. The sensitivity to damage was still greater in the Kautsky curves with the largest difference at 280 nm. Damage to PS II as calculated from DCMU induction curves was minimal at all wavelengths and in some instances the addition of UVA light actually enhanced $\phi_{IIe}{}^{\circ}$; even though the Kautsky measurements indicated damage. Subsequent changes in the σ_{psII} because of either decreases or increases in $\phi_{IIe}{}^{\circ}$ were outside of the resolution of the measurements (Table 2).

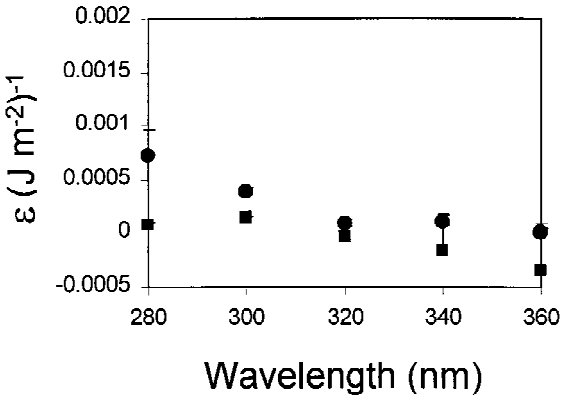

Figure 3. Action spectra of damage to $\phi_{IIeo(Kaut)}$ (circles) and $\phi_{IIeo(DCMU)}$ (squares) after a thirty minute incubation under monochromatic UVR and 60 μmol photons $m^{-2}\ s^{-1}$ PAR (error bars are the 95% confidence limits, $n > 4$).

UVR induced changes in photosynthetic function

Carbon fixation

The measurements of ϵ_H for carbon fixation after exposure to UV and PAR was wavelength dependent but not an exponentially decreasing function (Figure 4). Decreased rates of carbon fixation to *T. pseudonana* were maximal at 280 nm. Unlike polychromatic spectra of damage to carbon fixation no significant differences between the wavelengths 300 and 320 were found. The wavelength that induced the least damage was 360 nm. As was noted in the DCMU measurements under PAR and UVA there were occasional instances of enhancement in carbon fixation rates under UVA wavelengths.

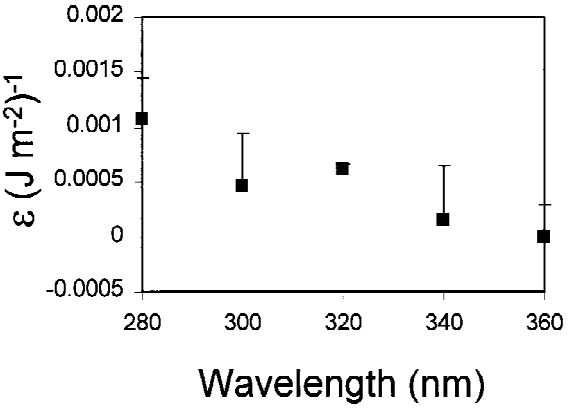

Figure 4. Action spectrum of damage to carbon fixation after a thirty minute incubation under monochromatic UVR and 60 μmol photons $m^{-2}\ s^{-1}$ PAR (error bars are the 95% confidence limits, $n > 4$).

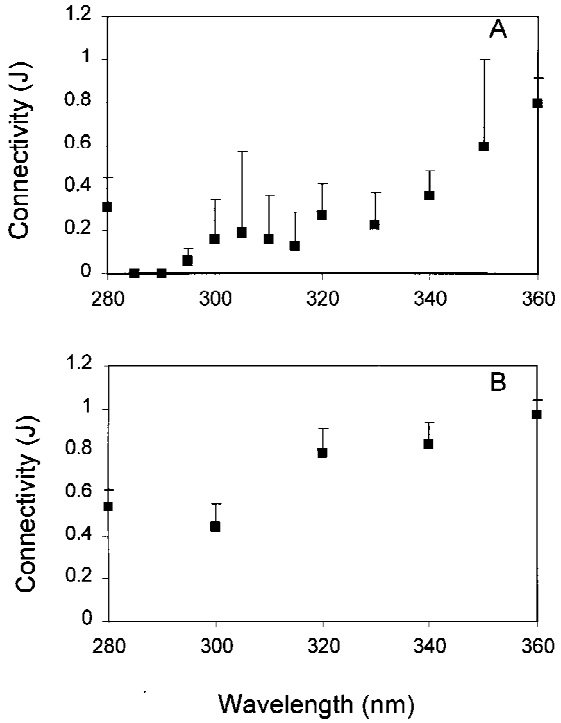

Figure 5. (A) Measurement of the parameter J_{con} as calculated from induction curves with DCMU after a thirty-minute incubation under monochromatic UVR only (error bars are the 95% confidence limits). (B) As in A, but after a 30 minute incubation under monochromatic UVR and 60 μmol photons m^{-2} s^{-1} PAR.

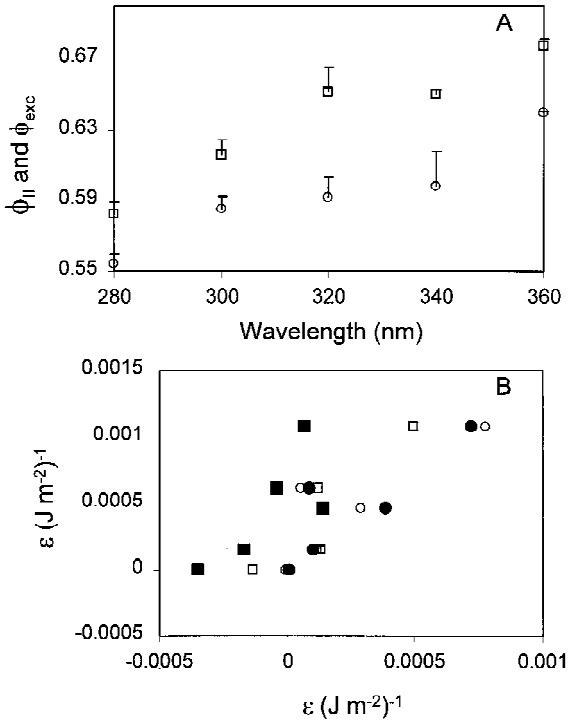

Figure 6. (A) Circles indicate measurements for the efficiency of photon trapping by PSII after a 30 minute incubation under monochromatic UVR and 60 μmol photons m^{-2} s^{-1} PAR (ϕ_{exc}) (error bars are the 95% confidence limits, $n > 4$). Squares indicate measurements for the apparent quantum yield of PS II (ϕ_{II}) after a 30 min incubation under monochromatic UVR and 60 μmol photons m^{-2} s^{-1} PAR (error bars as indicated above). Values of ϕ_{II} and ϕ_{exc} under PAR alone were 0.68 (0.005) and 0.63 (0.01), respectively. (B) The relationship between the weights ϵ as calculated from fluorescence parameters, $\phi_{IIe}{}^{\circ}{}_{(kaut)}$ (closed circle), $\phi_{IIe}{}^{\circ}{}_{(dcmu)}$ (closed square), ϕ_{II} (open square), and ϕ_{exc} (open circle) *versus* the weights ϵ as calculated from measurements of carbon fixation. The corresponding type II linear regressions of the slopes and R^2 values are presented in Table 3 for clarity.

Connectivity between reaction centers

Besides changes in $\phi_{IIe}{}^{\circ}$, exposure to UVR induced highly significant changes in the connectivity (J_{con}) between PS II reaction centers. Changes in J_{con} mimic the changes reported in both measurements of $\phi_{IIe}{}^{\circ}$; connectivity between reaction centers declines as damage increases. The most significant changes in J_{con} were induced by UVR alone at 285 and 295 nm, where there was no connectivity (Figure 5). This is also similar to the results found for decreases in $\phi_{IIe}{}^{\circ}$ where the greatest change was in the treatment with UVR only. In UVR and PAR treatments changes in J_{con} were minimal except at 280 and 300 nm.

PS II light utilization

The effects of UV light on PS II function in the presence of PAR and its possible relationship to changes in carbon fixation were assessed. Changes in the absolute values of both the operational quantum yield (ϕ_{II}) and the efficiency of photon trapping (ϕ_{exc}) are shown (Figure 6a). Decreases in both ϕ_{II} and ϕ_{exc} were consistent with the other measurements; damage increased as wavelength decreased. However, significant differences in the amount of damage between the two measurements exist. At all wavelengths damage as indicated by ϕ_{II} was greater than that indicated by ϕ_{exc} with the greatest differences at 320 and 340 nm.

In order to compare the relationship between $\phi_{IIe}{}^{\circ}{}_{(kaut)}$, $\phi_{IIe}{}^{\circ}{}_{(DCMU)}$, ϕ_{II}, $\phi_{exc,}$ and the changes in carbon fixation, all of the data are plotted according to the measurements of ϵ_H $(J\ m^{-2})^{-1}$ and the linear equations of the lines of best fit are shown in Table 3 (Figure 6b). The type II linear regression between ϕ_{II} and carbon fixation gives the line of best fit (R^2 = 0.81). While all of the linear regressions except for measurements with DCMU were good the slopes indicate that while damage to PS II and depressions in

Table 3. Parameters for type II linear regressions from the data in Figure 6B comparing the weightings of the fluorescence parameters to the damage to carbon fixation. Linear regressions were solved using a cubic equation and the standard deviations of the error in both the x and y directions. Values of the slope and Y-intercept are shown ± the 95% confidence interval

	Slope	Y-intercept	R^2
Kautsky w/ DCMU	3.78 ± 1.3	0.0006 ± 0.005	0.44
Kautsky w/o DCMU	1.43 ± 0.24	0.0002 ± 0.004	0.78
ϕ_{exc}	1.43 ± 0.25	0.0002 ± 0.004	0.77
ϕ_{II}	1.97 ± 0.30	0.0002 ± 0.0004	0.81

carbon fixation are linearly related they do not occur with a slope of one.

Changes in other fluorescence variables (σ_{psII}, K_a, K_b, a, and b) were highly variable and were generally not statistically significant from non-treated samples (Table 3). However, this can be assumed to be both a product of any effect the treatment had on the sample and a loss of computing power due to noise in the curves. Both are manifested in larger errors as wavelength decreases and damage increases.

Discussion

The difficulty in assessing actual targets of damage in the photosynthetic apparatus is caused both by multiple potential target sites and, over time, by an active repair cycle. We avoided some of the multiple potential target sites by using near monochromatic light. However, it is possible that different target sites have the same absorption maximum. As well, damage to the photosynthetic apparatus is often the result of cumulative dose affecting multiple processes simultaneously (Jones and Kok 1966; Baker and Bowyer 1994).

Photosynthesis, below the level of light saturation, is a product of irradiance, the number of reaction centers and the optical cross sections of PS II. We would expect damage to be a function of the efficiency of the wavelength at altering n or σ_{psII} and not a situation similar to that of dosage rate or bright light photoinhibition. In dosage rate photoinhibition, the efficiency and magnitude of damage is masked by repair and/or xanthophyll induced quenching so that in time a steady state is reached. During bright light photoinhibition, the incident flux, which is disproportionately high compared to the dissipative capacity of PS II, causes damage that is independent of the wavelength (Jones and Kok 1966). These phenomena will be species, time and acclimation state dependent. Given the monochromatic light regimes and the relatively low output at each wavelength ($\sim$150 J m^{-2}), these processes could be overlooked. Instead, the efficiency of damage could be investigated with the initial assumption that the plastoquinone pool would never be fully reduced and that any target sites impacting α would overwhelmingly be associated with PS II.

Although the increase in damage with decreasing wavelengths is not surprising (cf. Coohill 1991; Baker and Bowyer 1994; Lumsden 1997) the discrepancy between the various measurements can not simply be explained by the mechanics of the different measurements (Schreiber 1995; Kolber et al. 1998). The measurements were independent, highly repeatable and showed wavelength specific features. It is clear from Figure 6 that the fluorescence measurements agree well with the measurements of damage to carbon fixation even though the slopes of both lines indicate that the damage to PS II underestimates the overall damage to carbon fixation. An underestimation implies that not all of the damage to carbon fixation originates from PS II targets. However both the theoretical (as defined by Equations (5) and (6) and measured correlation ($R^2 \sim 0.77$) between damage to PS II and carbon fixation are robust. Discrepancies between PS II and carbon fixation damage would likely increase during light-saturated photosynthesis when the re-oxidation of the plastoquinone pool becomes a limiting factor to the maximum rate of photosynthesis. As well, if targets are located outside of PS II, the damage measured here is a low estimate of damage. It is also very clear from the comparisons of the damage to the quantum yield under UV light alone and under both UV and PAR that PAR light alleviates the damage to PS II. This is perhaps due to the reduction of molecules involved in radical scavenging. The comparisons of the yields of UV and UV/PAR treated phytoplankton demonstrate the rapid response to potential damage not withstanding the effects of photoactivation or active repair.

Changes in the quantum yield alone do not elucidate the mechanisms of damage associated with UVR. In fact, studies have been done showing little or no change in the quantum yield of PS II despite a large plant and microalgal literature implicating the D1 protein site as a potential target of damage (Neale et al. 1993; Lesser et al. 1994). This is because the correct interpretation of fluorescence measurements requires

considering both the time constants of the measurements and the specificity of the target site (Butler 1978; Geacintov and Breton 1987; Govindjee 1995). For example, the herbicide DCMU competes with plastoquinone for binding to the Q_B site, blocking electron transport from Q_A to Q_B. The DCMU induction curve therefore, gives information on the fraction of reduced Q_A (Melis and Duysens 1979; Melis and Schreiber 1979); it is not a good indicator of changes in either [Q_A] or [PQ]. The data show poor relationships between the damage as estimated from Kautsky curves with DCMU and without DCMU. The significant inconsistencies between damage to carbon fixation and changes in the quantum efficiency of PS II as calculated from the different fluorescent measurements suggest damage beyond the site of DCMU binding. Simply described the damage to PS II as indicated by the fluorescence transients reduces the electron flow from the reaction centre to plastoquinone.

Analysis of the DCMU induction rise shows significant wavelength dependency in the connectivity parameter J_{con} despite not seriously altering both $\phi_{IIe}{}^{\circ}{}_{(DCMU)}$ and the optical cross section of PS II. If a change in the concentration of oxidised Q_A was an important component of UV damage this should have been manifested as a change in either the amplitudes of the slow or fast components of the fluorescence decay curves after a single turnover saturating flash. However, no significant changes were found. Furthermore, we would have expected considerable variability in both $\phi_{IIe}{}^{\circ}{}_{(DCMU)}$ and the optical cross section of PS II if the D1 protein were a major UV target. Perhaps a change in the connectivity is a discrete mechanism that while not seriously altering σ_{psII}, provides oxidative relief through non-photochemical quenching (i.e. heat dissipation).

Despite small decreases in $\phi_{IIe}{}^{\circ}{}_{(DCMU)}$ and σ_{psII} these data show that exciton movement is impacted by UV, especially UVB. Unlike the cases of no UVR or when there is free exciton movement, an increase in UVR inhibits free distribution of energy among the reaction centers in a domain. The competition for excitation energy decreases because exciton movement is related to the functional distance between pigments (Paillotin 1976). These data suggest that high energy UVB causes a conformational change in the reaction center structure. This change results in either a small loss of efficiency of stable charge separation or an inability of the reaction center to dissipate exciton energy. Under low or no light conditions UV photons cause instability of $Q_B{}^-$. Our data on the differences in induction curve damage with and without DCMU would indicate that this causes a reduction in the rate of electron flow to PQ. This is also consistent with the increase in damage seen under no PAR light. In this case the potential of $Q_B{}^-$ to become reduced again, protonated and then exchanged with PQ is low. In other words, the addition of UVR makes light damage more efficient even under light limiting conditions by altering the function (ability to generate stable charge separation) but more importantly the physical structure of reaction centers (where the eventual result is decrease in the probability of reducing PQ).

The distinction between ϕ_{II} and ϕ_{exc} is based on the redox state of Q_A with ϕ_{exc} calculated from the maximum variable fluorescence under actinic light while ϕ_{II} is strongly influenced by the PFD (Kroon 1994). However, in the case of our measurements the PFD did not change so the increase in Ft is the result of UV light induced quenching (Equation 4, Figure 6a). As well, the discrepancy between ϕ_{exc} and either carbon damage or $\phi_{IIe}{}^{\circ}{}_{(Kaut)}$ indicates that damage is greater to F_m than $F_m{}'$. The net result is a decrease in the total electron transport as wavelength decreases. The light-limited, carbon fixation rate is dependent on this flow of electrons from PS II. Electron transport is the product of σ_{psII}, photon flux density (PFD) and ϕ_{II}. Our experimental setup held PFD constant and only small changes in σ_{psII} are reported. This would explain the robust relationship between ϕ_{II} and carbon damage. It should therefore be possible to draw conclusions about decreases in carbon fixation and potentially growth rate from measurements of ϕ_{II} and PFD. Furthermore, this non-invasive measurement is amenable to *in situ* studies of UV damage.

In conclusion, damage from UVR to either PS II or carbon fixation shows a wavelength dependency. Damage to the PS II quantum yields is robustly and linearly related to carbon fixation on short time scales. This relationship reflects damage at target sites on both the donor and acceptor side of PS II and can be explained by comparing the discrepancies between the different measurements of PS II fluorescence. Ultraviolet light decreases the electron flow from reaction centers to plastoquinone. Under light limiting conditions like those found in the oceans, this is significant.

Acknowledgements

The authors would like to thank Bruce Diner, Pat Neale and one anonymous reviewer for their com-

ments and suggestions. As well we thank Bernd Kroon for providing software to solve the fluorescence curves and Paul Falkowski, Zbigniew Kolber and Gennady Ananyev for their helpful discussions.

Appendix

F_o = Fluorescence yield when all Q_A is oxidised

F_m = Fluorescence yield when all Q_A is reduced

F_o' = Fluorescence yield when Q_A is oxidised after actinic illumination

F_m' = Fluorescence yield when Q_A is reduced by saturating light after actinic illumination

F_t = Fluorescence yield in the presence of actinic illumination

q = proportion of open PS II reaction centers

J_{con} = connectivity among reactions centers in PS II domains

σ ps II = geometric absorption cross section of the PS II reation center [relative units].
Units for σ are usually $þ^2$ (quanta); however, for the calculations here units are relative
to the incoming light which was constant in all instances

σ_{psu} = geometric absorption cross section of a photosynthetic unit that participated in the evolution
of one molecule of oxygen

A = amplitude of PS II that shows a fast fluorescence decay after a single turnover flash

B = amplitude of PS II that shows a slow fluorescence decay after a single turnover flash

k_a = Fast fluorescence decay rate constant [ms^{-1}]

k_b = Slow fluorescence decay rate constant [s^{-1}]

ϕ IIe°(DCMU) = Maximum quantum yield of PS II for stable charge separations as calculated from Kautsky induction
curves with DCMU

ϕ IIe°(kaut) = Maximum quantum yield of PS II for stable charge separations as calculated from Kautsky induction
curves without DCMU

ϕ_{exc} = Efficiency of photon trapping by open reaction centers of PS II in the presence of actinic illumination

ϕ_{II} = Apparent quantum yield of PS II for stable charge separations

ϕ_i = Fluorescence yield of the rise of the Kautsky curve from F_o to F_i

ϕ_d = Fluorescence yield of the rise of the Kautsky curve from F_o to F_d

ϕ_p = Fluorescence yield of the rise of the Kautsky curve from F_o to F_p, equivalent to $\phi_{IIe}°_{(kaut)}$

P_{max} = Maximum rate of carbon fixation [μg C μg Chl a^{-1} h^{-1}]

α = The light limited slope of the photosynthesis- irradiance relationship [μg C μg Chl a^{-1} h^{-1} (μmol m^{-2} s^{-1})$^{-1}$]

I_k = P_{max} / α, the irradiance at which P_{max} would be reached if photosynthesis was a linear function of photon flux [μmol m^{-2} s^{-1}]

References

Baker NR and Bowyer JR (1994) Photoinhibition of Photosynthesis from Molecular Mechanisms to the Field. BIOS Scientific, Oxford, 471 pp

Baker NR, Nogues S and Allen DJ (1997) Photosynthesis and photoinhibition. In: Lumsden P (ed) Plants and UVB: Responses to Environmental Change, pp 95–111. Cambridge University Press, Cambridge, UK

Boucher NP and Prezelin BB (1996) An *in situ* biological weighting function for UV inhibition of phytoplankton carbon fixation in the Southern Ocean. Mar Ecol-Prog Ser 144 (1–3): 223–236

Butler WL (1978) Energy distribution in the photochemical apparatus of photosynthesis. Annu Rev Plant Physiol 29: 345–378.

Caldwell MM, Camp LB, Warner CW and Flint SD (1986) Action spectra and their key role in assessing biological consequences of solar UV-B radiation change. In: Worrest RC and Caldwell MM (eds) Stratospheric Ozone Reduction, Solar Ultraviolet Radiation and Plant Life, pp 87–111. Springer-Verlag, New York

Calkins J and Thordardottir T (1980) The ecological significance of solar UV radiation on aquatic organisms. Nature 283: 563–566

Cao J and Govindjee (1990) Chlorophyll *a* fluorescence transient as an indicator of active and inactive Photosystem II in thylakoid membranes. Biochim Biophys Acta 1015: 180–88

Coohill TP (1989) Ultraviolet action spectra for higher plants. Photochem Photochem 50: 451–457

Coohill TP (1991) Action spectra again? Photochem. Photobiol 54: 859–870

Cullen JJ and Lesser MP (1991) Inhibition of photosynthesis by ultraviolet radition as a function of dose and doseage rates: Results for a marine diatom. Mar Biol 111: 183–190

Cullen JJ, Neale PJ and Lesser MP (1992). Biological weighting function for the inhibition of phytoplankotn photosynthesis by ultraviolet radiation. Science 258: 646–650

Diner BA and deVitry C (1985) In: Sybesma C (ed) Advances in Photosynthesis Research, Vol 1, pp 407–411. Martinus Nijhoff/Dr W. Junk, The Hague.

Dionisio ML, Tsuzuki M and Miyachi S (1989) Blue light induction of carbonic anydrase activity in *Chlamydomonas reinhardtii*. Plant Cell Physiol 30: 215–219

El-Sayed SZ, Stephens FC, Bidigare RR and Ondrusek ME (1990) Effect of ultraviolet radiation on Antarctic marine phytoplankton. In: Kerry KR and Hempel G (eds) Antarctic Ecosystems. Ecological Change and Conservation, pp 379–85. Springer-Verlag, Berlin

Farman JC, Gardiner BG and Shanklin JD (1985) Large losses of total ozone in Antarctica reveal seasonal ClOx/NOx interaction. Nature 328: 207–210

Geacintov NE and Breton J (1987) Energy transfer and fluorescence mechanisms in photosynthetic membranes. CRC Crit Rev Plant Sci 5: 1–44

Govindjee (1995) Sixty-three years since Kautsky: Chlorophyll a flourescence. Aust J Plant Physiol 22: 131–160

Greenberg BM, Gaba V, Canaani O, Malkin S, Mattoo AK and Edelman M (1989) Separate photosensitizers mediate degradation of

the 32-kDa photosystem II reaction center protein in the visible and UV spectral regions. Proc Natl Acad Sci 86: 6617–6620

Guillard RRL (1975) Culturing of phytoplankton for feeding marine invertebrates. In Smith WL and Chanley MH (eds) Culture of Marine Invertebrate Animals, pp 29–60. Plenum Press, New York

Helbing EW, Villafane V, Ferrario M and Holm-Hansen O (1992) Impact of natural ultraviolet radiation on rates of photosynthesis and on specific marine phytoplankton species. Mar Ecol Prog Ser 80: 89–100

Iwanzik W, Tevini M, Dohnt G, Voss M, Weiss W, Graber P and Renger G (1983) Action of UV-B on photosynthetic primary reactions in spinach chloroplasts. Physiol Plant 58: 401–07

Jansen MAK, Gaba V, Greenberg B, Mattoo KA and Edelman M (1993) UV-B driven degradation of the D1 reaction-center protein of Photosystem II proceeds via plastosemiquinone. In: Yamamoto HY and Smith CM (eds) Photosynthetic Responses to the Enivronment, pp 142–49. American Society of Plant Physiologists, Rockville, Maryland

Jeffrey SW and Humphrey GF (1975) New spectrophotometric equations for determining chlorophylls a, b, c1 and c2 in higher plants, algae and natural phytoplankton. Biochem Physiol Pflanzen 167: 191–194

Jokiel PL and York RH Jr. (1984) Importance of ultraviolet in photoinhibition of microbial growth. Limnol Oceanogr 29: 192–99

Jones LW and Kok B (1966) Photoinhibition of chloroplast reactions. I. Kinetics and action spectra. Plant Physiol 41: 1037–1043

Karentz D (1994) Ultraviolet tolerance mechanisms in Antarctic marine organisms. In: Weiler S and Penhale P (eds) Ultraviolet Radiation in Antarctica: Measurements and Biological Effects. Ant Res Ser 93–110

Karentz D, Cleaver JE and Mitchell DL (1991) Cell survival characteristics and molecular responses of Antarctic phytoplankton to ultraviolet-B. J Phycol 27: 326–341

Kolber ZS, Prasil O and Falkowski PG (1998) Measurements of variable fluorescence using fast repetition rate techniques: defining methodology and experimental protocols. Biochim Biophys Acta 1367: 88–106

Kroon BMA (1994) Variability of Photosystem II quantum yield and related processes in *Chlorella pyrenoidosa* (Chlorophyta) acclimated to an oscillating light regime simulating a mixed photic zone. J Phycol 30: 841–852

Kulandaivelu G and Noorudeen AM (1983) Comparative study of the action of ultraviolet-C and ultraviolet-B radiation on photosynthetic electron transport. Physiol Plant 58: 389–94

Lavorel J (1959) Induction of flourescence in quinone-poisoned *Chlorella* cells. Plant Physiol 34: 204–209

Lesser MP, Cullen JJ and Neale PJ (1994) Carbon uptake in a marine diatom during acute exposure to ultraviolet B radiation: Relative importance of damage and repair. J Phycol 30: 183–92

Lumsden PJ (ed) (1997) Plants and UVB: Responses to Environmental Change. Cambridge University Press, Cambridge, UK, 355 pp

Melis A and Duysens LNM (1979) Biphasic energy conversion kinetics and absorbance difference spectra of Photosystem II of chloroplasts. Evidence for two differnent photosystem II reaction centers. Photochem Photobiol 29: 373–382

Melis A, Nemson JA and Harrison MA (1992) Damage to functional components and partial degradation of Photosystem II reaction center proteins upon chloroplast exposure to ultraviolet-B radiation. Biochim Biophys Acta 1100: 312–20

Melis A and Schreiber U (1979) The kinetic relationship between the c-550 absorbance change, the reduction of Q (A320) and the variable fluorescence yield change in chloroplasts at room temperature. Biochim Biophy Acta 547: 47–57

Munday JCM Jr and Govindjee (1969) Light-induced changes in the fluorescence yield of chlorophyll a *in vivo*. III. The dip and peak in fluorescence transient of *Chlorella pyrenoidosa*. Biophy J 9: 22–33

Neale PJ and Kieber DJ (2000) Assessing biological and chemical effects of UV in the marine environment: spectral weighting functions. In: Hester RE and Harrison RM (eds) Causes and Environmental Implications of Increased UV-B Radiation. Issues in Environmental Science and Technology, No 14, pp 61–83. The Royal Society of Chemistry, Cambridge

Neale PJ, Cullen JJ, Lesser MP and Melis A (1993) Physiological bases for detecting and predicting photoinhibition of aquatic photosynthesis by PAR and UV radiation. In: Yamamoto HY and Smith CM (eds) Photosynthetic Responses to the Enivronment. pp. 61–77 American Society of Plant Physiologists, Rockville, Maryland

Neale PJ, Davis RF and Cullen JJ (1998) Interactive effects of ozone depletion and vertical mixing on photosynthesis of Antarctic phytoplankton. Nature. 392: 585–589

Neale PJ, Lesser MP and Cullen J J (1994) Effects of ultraviolet radiation on the photosynthesis of phytoplankton in the vicinity of McMurdo station, Antarctica. In: Weiler S and Penhale P (eds) Ultraviolet Radiation in Antarctica: Measurements and Biological Effects. Ant Res Ser 125–142

Ohad I, Keren N, Zer H, Gong H, Mor T, Gal A, Tal and DY (1994) Light – induced degradation of the Photosystem II reaction centre D1 protein *in vivo*: an integrative approach. In: Baker NR and Bowyer JR (eds) Photoinhibition of Photosynthesis from Molecular Mechanisms to the Field, pp 161–177. BIOS Scientific, Oxford

Paillotin G (1976) Movements of excitations in the photosynthetic domains of Photosystem II. J Theor Biol 58: 237–252

Prézelin BB, Boucher NP and Schofield O (1994a) Evaluation of field studies of UVB radiation effects on Antarctic marine primary production. In: Biggs RH and Joyner MEB (eds) Stratospheric Ozone Depletion: UV-B Radiation in the Biosphere. NATO ASI Series 118: 181–94

Prézelin BB, Boucher NP and Smith RC (1994b) Marine primary production under the influence of the Antarctic ozone hole: Icecolors 90. In: Weiler S and Penhale P (eds) Ultraviolet Radiation in Antarctica: Measurements and Biological Effects. Ant Res Ser 159–186

Quaite FE, Sutherland BM and Sutherland JC (1992) Action spectrum for DNA damage in alfalfa lowers predicted impact of ozone depletion. Nature 358: 576–578

Renger G, Völker M, Eckerty HJ, Fromme R, Hom-Veit S and Gräber P (1989) On the mechanism of Photosystem II deterioration by UV-B radiation. Photochem Photobiol 49: 97–105

Richter M, Rühle W and Wild A (1990) Studies on the mechanism of Photosystem II photoinhibition I. A two-step degradation of D1-protein. Photosynthesis Res. 24: 229–35

Rundel RD (1983) Action spectra and estimation of biologically effective UV radiation. Physiol Plant 58: 360–366

Sakshaug E, Bricaud A, Dandonneau Y, Falkowski PG, Kiefer DA, Legendre L, Morel A, Parslow J and Takahashi M (1997) Parameters of photosynthesis: Definitions, theory and interpretation of results. J Plank Res 19(11): 1637–1670

Savitsky A and Golay MJ (1964) Smoothing and differentiation of data by simplified least squares procedure. Anal Chem 36: 1627–1638

Schnettger B, Critchley C, Santore U J, Graf M and Krause GH (1994) Relationship between photoinhibition of photosynthesis,

D1 protein turnover and chloroplast structure. Effects of protein synthesis inhibitors. Plant Cell Environ 17: 55–64

Schofield O, Prézelin BB and Kroon BMA (1995) Impact of ultraviolet-B radiation on Photosystem II activity and its relationship to the inhibition of carbon fixation rates for Antarctic ice algae communities. J Phycol 31: 703–715

Schreiber U, Hormann H, Neubauer C and Klughammer C (1995) Assessment of Photosystem II photochemical quantum yield by chlorophyll fluorescence quenching analysis. Aust J Plant Physiol 22(2): 209–220

Smith RC, Baker K, Holm-Hansen O and Olson RS (1980) Photoinhibition of photosynthesis in natural waters. Photochem Photobiol 31: 585–592

Smith RC, Prezelin BB, Baker KS, Bidigare RR, Boucher NP, Coley T, Karentz D, MacIntyre S, Matlick HA, Menzies D, Ondrusek M, Wan Z and Waters KJ (1992) Ozone depletion: Ultraviolet radiation and phytoplankton biology in Antarctic waters. Science 255: 952–959

Strid A, Chow WS and Anderson JM (1990) Effects of supplementary ultraviolet-B radiation on photosynthesis in *Pisum sativum*. Biochim Biophys Acta 1020: 260–68

Trissl H-W and Lavergne J (1994) Fluoresence induction from Photosystem II: analytical equations for the yields of photochemistry and fluorescence derived from analysis of a model including exciton-radical pair equilibrium and restricted energy transfer between photosynthetic units. Aust J Plant Physiol 22: 183–193

Teramura AH, Ziska LH and Sztein AE (1991) Changes in growth and photosynthetic capacity of rice with increased UV-B radiation. Physiol Plant 83: 373–380

Vass I, Sass L, Spetea C, Bakou A, Ghanotakis D and Petrouleas V (1996) UV-B-induced inhibition of Photosystem II electron transport studied by EPR and chlorophyll fluorescence. Impairments of donor and acceptor side components. Biochemistry 35(27): 8964–8973.

Vernet M, Brody EA, Holm-Hansen O and Mitchell BG (1994) The response of Antarctic phytoplankton to ultraviolet radiation: Absorption, photosynthesis, and taxonomic composition. In: Weiler S and Penhale P (eds) Ultraviolet Radiation in Antarctica: Measurements and Biological Effects. Ant Res Ser 143–158

Ziska LH, Teramura AH, Sullivan JH (1983) Physiological sensitivity of plants along an elevational gradient to UV-B radiation. Am J Bot 79(8): 863–871